“Babeş Bolyai” University

Cluj-Napoca

Faculty of Physics

Doctoral Thesis Summary

STRUCTURAL STUDIES ON NEW MATERIALS WITH POSSIBLE APPLICATION IN DOSIMETRY

Ionuț Cătălin Ivaşcu

Scientific Supervisor,

Prof. Dr. Onuc Cozar

Cluj-Napoca

2012

Content

Key words:

Phosphate glass

Raman spectroscopy

IR spectroscopy

Thermoluminescence

ESR

INTRODUCTION

Nowadays, the study of the phosphate glasses represents a special part in the large field of material science because of their applications in the different domains.

Many researchers have been focused on the phosphate glasses study over the last years due to theirs diversified applications in technology, medicine, as biomaterials and in clinical dosimetry. The phosphate glasses are often used as biomaterials since they are similar in chemical composition to the natural bone.

The aim of the present PhD thesis is the study of the structure and properties of glasses, which have P_2O_5 as glass former, with different modifiers of vitreous network, like BaO, CdO, Li_2O, with the purpose of developing a suitable material for dosimetric measurements.

In the first chapter theoretical information about obtaining and characterization of vitreous systems and a detailed description of the phosphate glass structure are presented.

The second chapter describes IR and Raman spectroscopy and their role in the study of oxides materials with vitreous structure. Furthermore, specific ways of studying and interpreting IR and Raman spectra are presented, as it is known that they generally contain large bands which are hard to interpret.

Chapter three presents the thermoluminescence phenomenon, the used equipment and theoretical aspects about thermoluminescence dosimetry.

In Chapter four structural aspects of the system $0.5P_2O$ - xBaO - (0.5-x) Li_2O using IR and Raman spectroscopy are analyzed, as well as its dosimetric properties of thermoluminescence measurements. The most important results are highlighted, which constitute new scientific contribution in the study of phosphate glasses.

Chapter five presents the results obtained by IR, Raman and ESR on the glass system P_2O_5-Li_2O-CdO where the P_2O_5 ratio remains constant 50mol% when Li_2O and CdO ranges from 0 - 50mol%.

The last chapter describes the structural aspects of the system $0.5P_2O_5$-xBaO-(0.5-x) K_2O, where $0 \leq x \leq 0.5$ mol%, through IR and Raman spectroscopy. Moreover, the effects of the modifiers oxides BaO and K_2O in the phosphate glasses matrix on thermoluminescence properties of these materials, together with their dosimetric properties of thermoluminescence measurements have been investigated.

CHAPTER 1

Oxide materials with vitreous state

The oxides acids - network creator- play a key role in achieving structural skeleton of the glass. For this reason, they are the glass's components with the largest quantities.

Basic oxides - network modifiers - do not contribute to the formation of vitreous network structural skeleton, but their positive ions destroy the vitreous network by creating gaps in time, break the links between basic structural units by changing the properties of the network. These oxides stabilize the disordered structure of the glass, ensuring its resistance to external factors, such as water, acids and other chemicals. This includes oxides as Na_2O, K_2O, Li_2O, CaO, MgO, PbO [1].

Recent studies have shown dual behavior of some oxides, of modifiers, as well as network creators according to the vitreous glass composition and the proportion in which they are found. Some of these oxides are: PbO, MoO_3, WO_3, V_2O_5, Fe_2O_3.

It can be said that the network is dominated by the relationship between the phosphate PO_4 tetrahedral. In case of the vitreous P_2O_5 structures, they are connected to adjacent structural units in three of the four links. Although the structure of phosphate glasses changes with the addition of the modifier oxides, phosphorus keeps its square coordination over the full range of compositions [2-10].

Phosphate glasses are the only oxide glasses for which the polymer structure has been experimentally determined. Besides this polymer structure, a common characteristic of phosphate glasses is the high complexity of structure, which involves a large number of polymeric species in the presence of a structurally dependent chemical equilibrium.

CHAPTER 2

Basis of vibrational spectroscopy

Spectroscopy in the infrared (IR) is the best method to identify the presence of polar functional groups of organic compounds molecular structure.

Infrared radiation (IR) is the part of the electromagnetic spectrum between visible and microwave region, which is characterized by wavelengths of order 10^{-5} m [11].

IR spectra have their origins in the transitions between atomic energy levels of different groups and are observed when forming the absorption spectra.

In the IR spectra two types of vibration of functional groups in a molecule can be identified, such as **stretching vibration** and **deformation vibration** (bending, rocking, wagging and twisting).

Raman effect is caused by changes in the distribution of electronic load under the effect of applied electromagnetic radiation, not by changes of the nuclear load distribution in the molecule. Additionally, from both experimental and practical points of view, the investigated sample should be exposed to an intense monochromatic beam, conditions met by a laser beam. For the same molecular species, the Raman spectrum greatly varies from the IR one in terms of intensity, the position and shape of the bands assigned to the same vibration [12-16].

CHAPTER 3

Thermoluminescence of phosphate glasses

Two phases can be defined in the thermoluminescence phenomenon [17-19]:

The irradiation phase:

When coming of the energy bands, the energy levels of crystals' defects are located inside the local level band gap. The irradiations produce the ionization of the environment. Therefore free electrons can appear in material. This is equivalent to the transfer of electrons from the valence band to the conduction band (phenomenon represented in Fig. 1. by 1). These electrons are free to move through the crystal until they are captured by certain defects (processes represented by 2, 3).

The production of free electrons is associated with the generation of free goals that behave as positive charges, which can also migrate, in terms of energy, through the valence band until they are captured by traps goals (processes 2 'and 3'). Many traps goals are thermally unstable even at room temperature and they can switch back into the valence band (4 '). Captured electrons will remain in some of the traps for a sufficiently long time if they do not get an energy overplus.

The heating phase:

The captured electrons on the metastabile levels can gain energy by reaching the conduction band. From this moment, they can undergo into the following processes: recapture the defects, fall into the valence band, radiative recombination with a hole in a luminescent center. Through the recombination of electrons with holes in luminescence centers (process 5), the excess energy is emitted as either UV or VIS radiation.

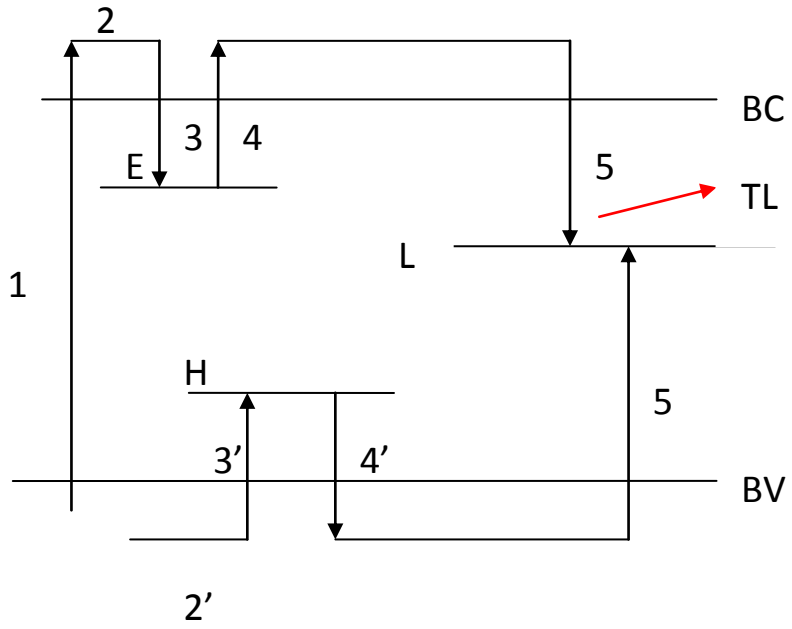

Fig. 1. Procese produse la iradierea şi încălzirea unui fosfor

CHAPTER 4

Vitreous glass system $0.5P_2O_5$-xBaO-$(0.5-x)Li_2O$

4.1. Sample preparation

The starting materials for obtaining $0.5P_2O_5$ - xBaO - $(0.5-x)Li_2O$ glass system with $0 \leq x \leq 50$ mol% were $(NH_4)_2HPO_4$, $BaCO_3$ and $LiCO_3$ of reagent grade purity. The samples were prepared by weighing suitable proportions of the components, powder mixing and mixture melting in sintered corundum crucibles at 1200 °C for one hour. The mixture was put into the furnace directly at this temperature. The obtained glass-samples were quenched by pouring the molten glass on a stainless steel plate.

4.2. IR study of $0.5P_2O_5$-xBaO-$(0.5-x)Li_2O$ glass system

Typical infrared spectra of studied glasses are shown in Fig.2. As seen from this figure, the frequencies of predominant absorption peaks are characterized by two broad peaks near 500 cm^{-1}, one weak peak around 770 cm^{-1}, three peaks in the 900-1270 cm^{-1} region and a weak peak around 1625 cm^{-1}.

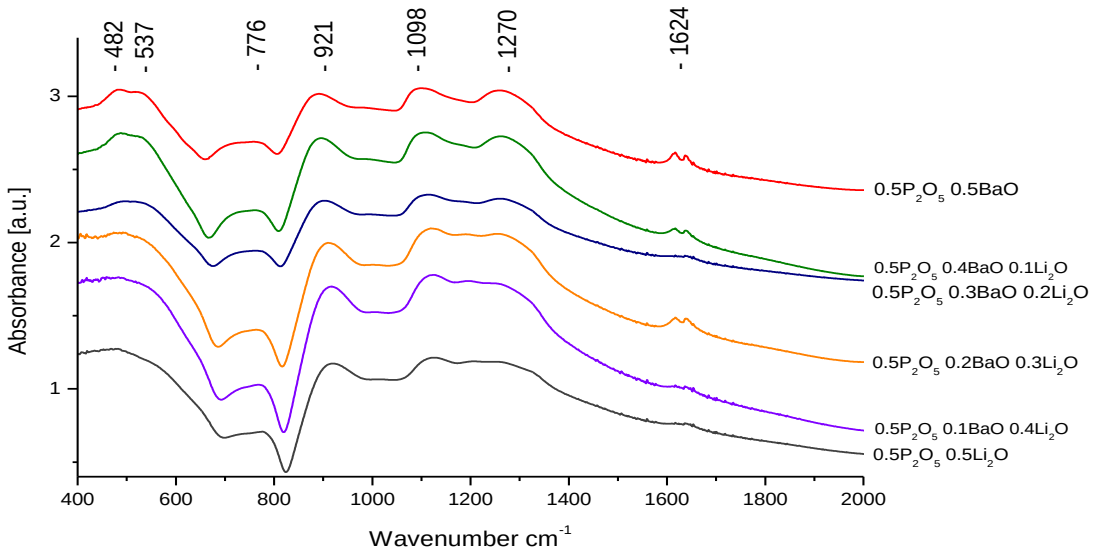

Fig. 2. IR spectra of $0.5P_2O_5 \cdot$xBaO $(0.5-x)Li_2O$ glass system with $0 \leq x \leq 0.5$ mol%

IR analyses reveal that the low frequency which envelope around 500 cm^{-1} consists of two component bands at ~482 and ~537 cm^{-1} respectively [20]. The band at about 482 cm^{-1} is

assigned as the bending vibrations of O-P-O units, $\delta(PO_2)$ modes of $(PO_2^-)n$ chain groups, and the band at ~537 cm^{-1} is described as a fundamental frequency of (PO_4^{3-}) or as harmonics of P=O bending vibrations [21-23]. The band from 776 cm^{-1}, may be attributed to the symmetric stretching vibration of P-O-P rings [24]. The variation of the frequency of P-O-P bonds with increasing Li_2O is in consistent with breakage of cyclic P-O-P bonds in the glass when the lithium oxide act as network modifier and band is shifted lower frequency. The absorption band at 921 cm^{-1} is attributed to asymmetric stretching vibration of P-O-P groups linked with linear metaphosphate chain [22, 23, 25]. The band at ~1098 cm^{-1} is assigned to asymmetric stretching of PO_2^- group, $\upsilon_{as}(PO_2^-)$ modes [22, 24]. The considerable shift in the position of this band toward higher wavenumber 1112 cm^{-1} and the increase in its relative area with increasing Li_2O content may be considered as an indication for the formation of the terminal phosphate groups, PO_3^{2-} .The broad features of the 1270 cm^{-1} band is attributed to the stretching of the doubly bonded oxygen vibration, υ_{as}(P=O) modes [22, 25].

4.3. Raman study of $0.5P_2O_5$-xBaO-(0.5-x)Li_2O glass system

It is known that usually the Raman spectra of phosphate glasses can be divided in two regions around ~700 cm^{-1} and ~1200 cm^{-1} [26, 27]. The bands from ~700 cm^{-1} corresponds to the bridging stretching modes and that at ~1200 cm^{-1} is ascribed to the terminal P–O stretching vibrations. Except of these two regions bands in the Raman spectra, the phosphate glasses can be observed often in other supplementary bands under 600cm^{-1}. These signals are due to the well-known boson peaks and to the complicated internal vibrations such as the skeletal deformation vibrations of phosphate chains and PO_3 deformation vibrations of pyrophosphate segments [28, 29].

Our Raman glasses spectra present five bands (Fig.3) : the first one at ~335 cm^{-1} is attributed to skeletal deformation vibrations of phosphate chains and PO_3 deformation vibrations of pyrophosphate segments [29], the second one at ~528 cm^{-1} corresponds to the bending mode related to the cation motion and chain structure[30], the third one at ~692 cm^{-1} is attributed to the symmetric stretching mode of P-O-P bridging oxygens, $(POP)_{sym}$, between Q^3 phosphate tetrahedra, the fourth one at ~1156 cm^{-1} is attributed to the symmetric stretching mode of O-P-O non-bridging oxygens, $(PO_2)_{sym}$, indicating the formation of Q^2 phosphate tetrahedral [31] and the last fifth band at ~1241 cm^{-1} is attributed to the symmetric stretch of the P=O terminal oxygens, $(P=O)_{sym}$ [27, 32].

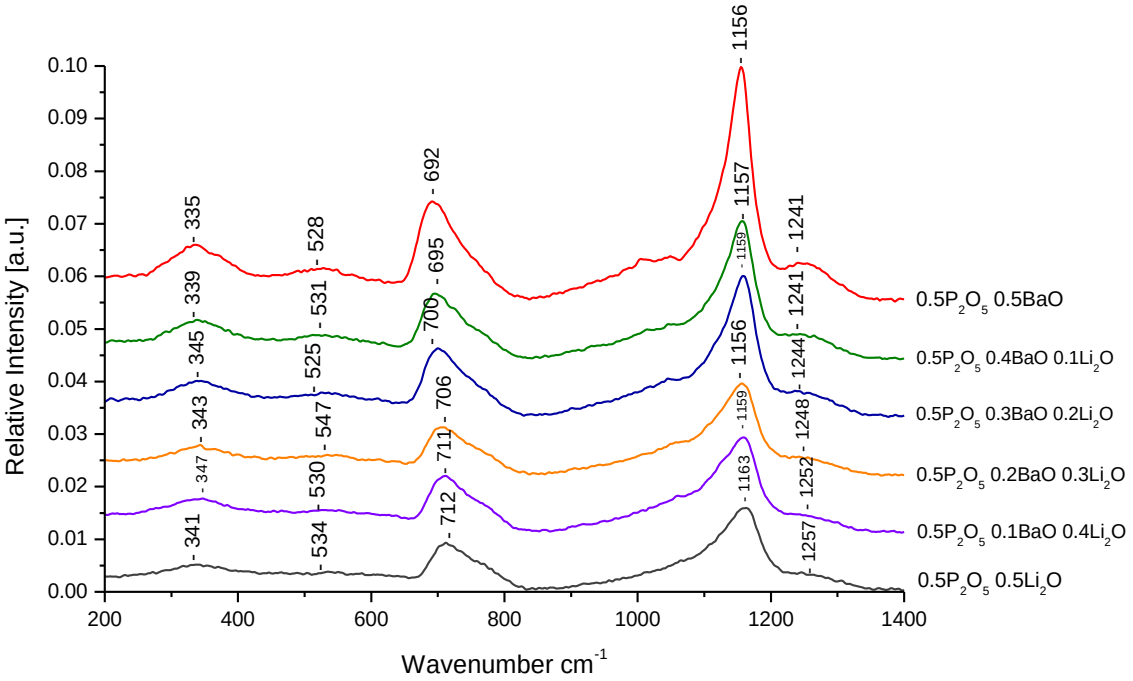

Fig. 3. Raman spectra of $0.5P_2O_5 \cdot xBaO\ (0.5\text{-}x)Li_2O$ glass system with $0 \leq x \leq 50$ mol%

The bands from 692 cm^{-1} and 1156 cm^{-1} are specific to phosphate glasses, but the assignment of the band centered at ~1241 cm^{-1} represents a problem. Based on several studies of $\nu\text{-}P_2O_5$ found in literature, Hudgens at al. [32] studied the structure of lithium ultraphosphate glasses. It was observed that the band assigned to P=O terminal oxygens, centered at ~1390 cm^{-1}, decreases in wavenumber to ~1250 cm^{-1} with the increasing of the alkali oxide from 20 to 50 mol% and became indistinguishable from the $(PO_2)_{asym}$ mode of a Q^2 tetrahedron. The explanation was that this decreasing in wavenumber is due to an increase in average length of the P=O bond resulting from π-bond delocalization on the Q^3 tetrahedra [32].

4.4. Thermoluminescence study of $0.5P_2O_5$-xBaO-$(0.5\text{-}x)Li_2O$ glass system

Luminescence emissions have been registered under a controlled heating rate of 5 $^oC/s$ immediately after 25 Gy of β irradiation. Simple phosphate glasses exhibited no TL signals. At least two peaks can be easily observed in the case of $0.5P_2O_5$ -0.5BaO freshly irradiated glass, one centered on 200 ^oC and a higher temperature peak at about 400 ^oC, while in the case of 0.5 P_2O_5 - 0.5 Li_2O the TL peak is centered at about 250 ^oC (Fig. 4.) [33].

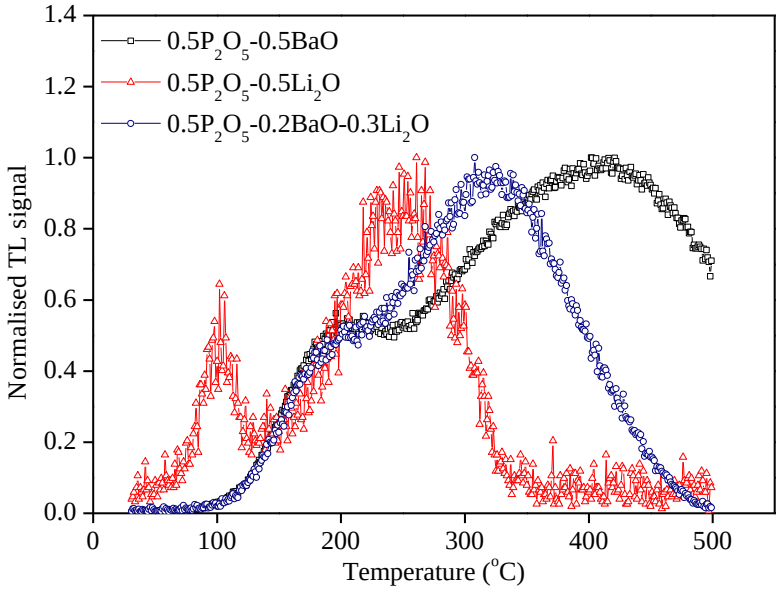

Fig. 4. Comparison of TL glow curves of P_2O_5 glass systems doped with different concentrations (0.5, 0.5, 0 mol %) of BaO and Li_2O.

In the case of $0.5P_2O_5$ - x BaO - (0.5-x) Li_2O glass systems with $10 \leq x \leq 40$ mol% TL emissions are consisting of the above-mentioned peaks overlapping, while P_2O_5 shows no TL signals. Thus, it can be inferred that the observed TL peaks correspond to different defects generated by the modifier ions (Ba^{+2}, respectively Li^{+1}) inserted into the glass network [33].

The dose response of TL signals for 0.5 P_2O_5 - 0.5 BaO and 0.5 P_2O_5 - 0.5 Li_2O glass systems are presented in Fig. 5. Fig. 6. respectively Fig. 8..

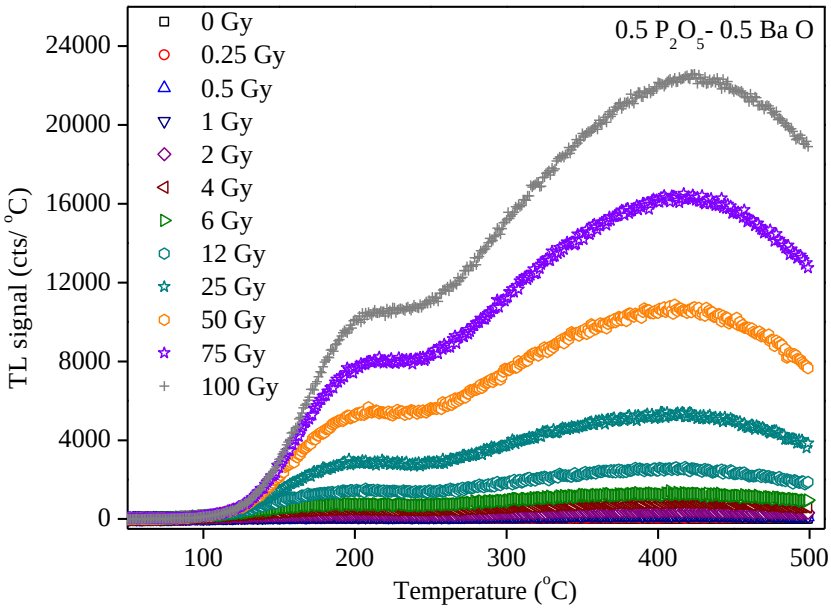

Fig. 5. TL glow curves of 0.5 P_2O_5 – 0.5 BaO glass freshly irradiated (^{90}Sr- ^{90} Y) to doses ranging from 0 to 100 Gy.

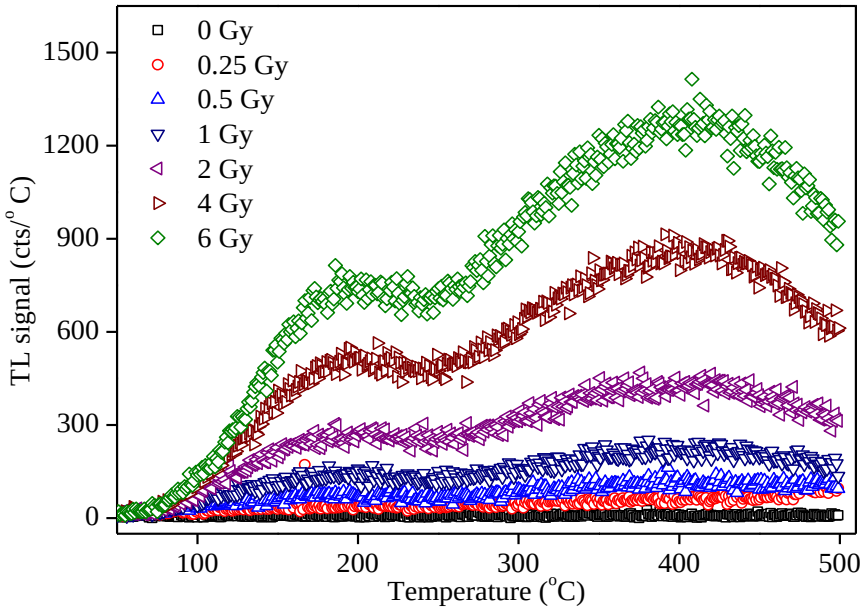

Fig. 6. TL response from Fig. 5. for relatively low doses (0-6 Gy).

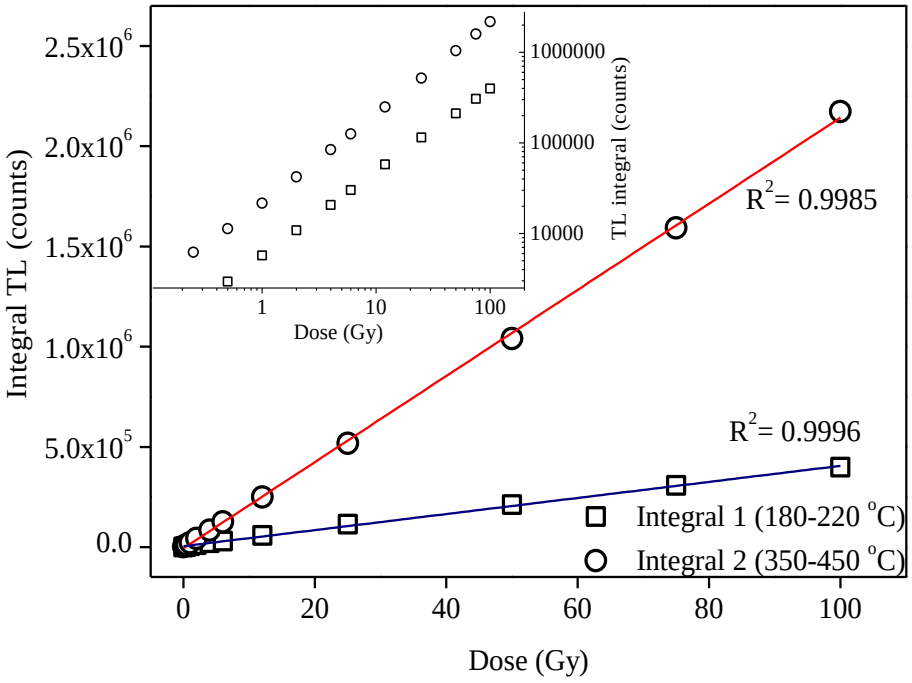

Fig. 7. Integral TL output (180-220 °C respectively 350-450 °C) as function of given dose. The inset presents the same data on a log-log scale. All measurements have been performed on one aliquot.

All measurements have been performed on a single aliquot for each glass specimen, as it was observed that the process of recording the TL signal (ramp heating to 500 °C) reduces all signals to a negligible level (3% of the response recorded after an irradiation of 10Gy). The

phosphate glass doped with barium oxide is one order of magnitude more sensitive than the one doped with lithium oxide. Based on twelve aliquots analysed it was concluded that for 1 gram of 0.5 P_2O_5 - 0.5 BaO glass the high temperature peak is approximately 50 times less sensitive than the traditional LiF:Mg, Ti (TLD 100) pellets for the above described experimental facility setup. However, a very good linear dependence ($R^2 > 0.99$) of the integral TL signal with dose can be observed for both dosimetric peaks of 0.5 P_2O_5 - 0.5 BaO up to at least 100Gy (Fig. 7.) [34]. As generally supralinearity is a characteristic of a large variety of TL materials in the dose region over 10 Gy [35], this characteristic makes the investigated material extremely attractive for high dose measurements.

On the other hand, the dependence of the integral TL signal (220 -320 ^oC) as function of given dose for 0.5 P_2O_5 - 0.5 Li_2O was observed to be superlinear (a quadric dependence) (Fig. 9.). This might indicated that the observed luminescence process is more complex than the first order kinetics [36]. Due to this fact, the subsequent investigations of dosimetric properties were focused on 0.5 P_2O_5 - 0.5 BaO glass.

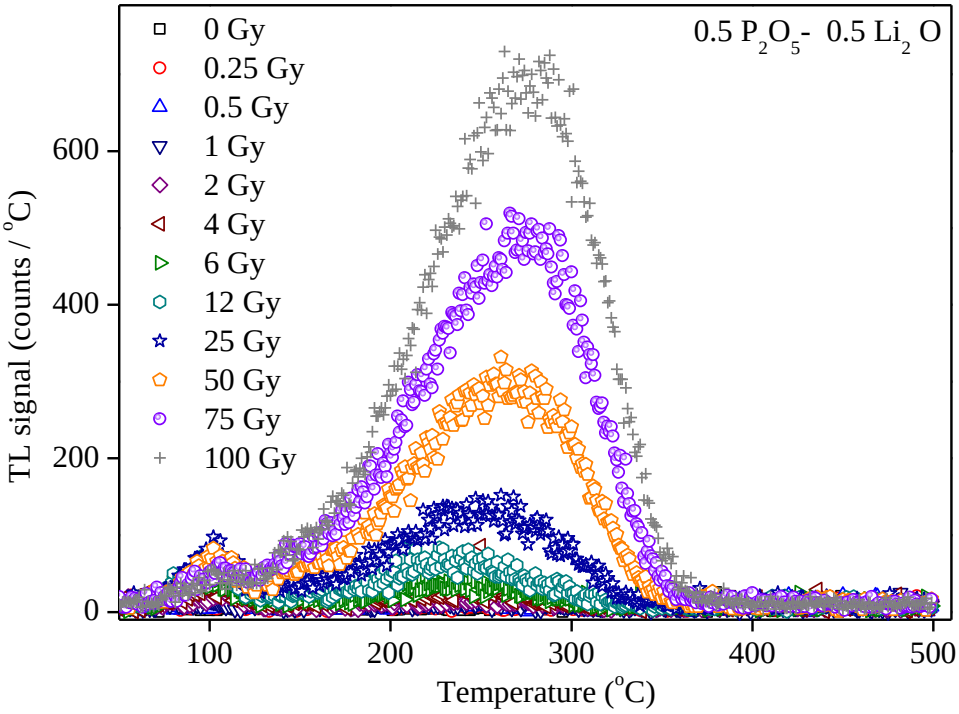

Fig. 8. TL glow curves of 0.5 P_2O_5 -0.5 Li_2O glass freshly irradiated (^{90}Sr- ^{90}Y) to doses ranging from 0 to 100 Gy.

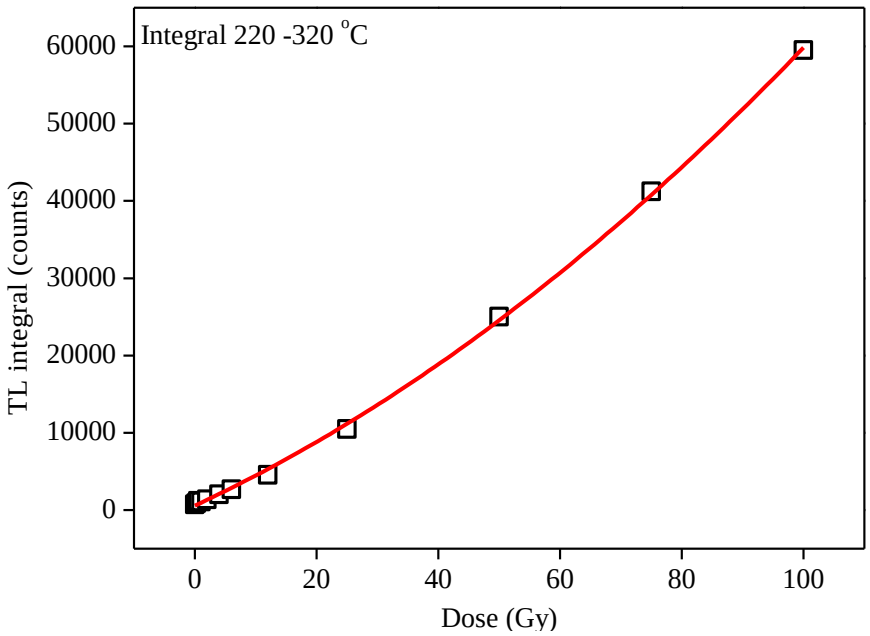

Fig. 9. Integral TL response (220 -320 °C) as function of given dose.

In order to test batch homogeneity, a set of 10 aliquots of 0.5 P_2O_5 - 0.5 BaO glass samples have been irradiated in a homogenous gamma field with a dose of 20 Gy. Luminescence measurements have been performed immediately after irradiation. The integral TL output (180-220 °C, 350-450 °C) was normalized to the mass of each aliquot. For the dosimetric peak at about 200 °C an average signal of 1257 cts/ mg was obtained, with a relative standard deviation of 9.8%, while in the case of the second dosimetric peak (350 ^{0}C) an average of 5410 cts/ mg was obtained with a relative standard deviation of 8.1%. Corresponding uniformity indexes have been quantified according to Furetta et al. (1998) [37]:

$$\Delta = [(M_{max} - M_{min}) / M_{min}] \cdot 100$$

where $M_{max,}$ respectively M_{min} represent the maximum and minimum values recorded. The determined values were 32, respectively 24 for the high temperature peak, indicating the homogeneity of the batch ($\Delta < 30$).

Reproducibility tests have been carried on twelve aliquots, each aliquot being repeatedly irradiated and heated to 500 °C over the course of three months. The average behavior of 12 aliquots over 10 measurement cycles is presented in Fig. 10.. None of the investigated aliquots showed a specific sensitization or desensitization trend [33].

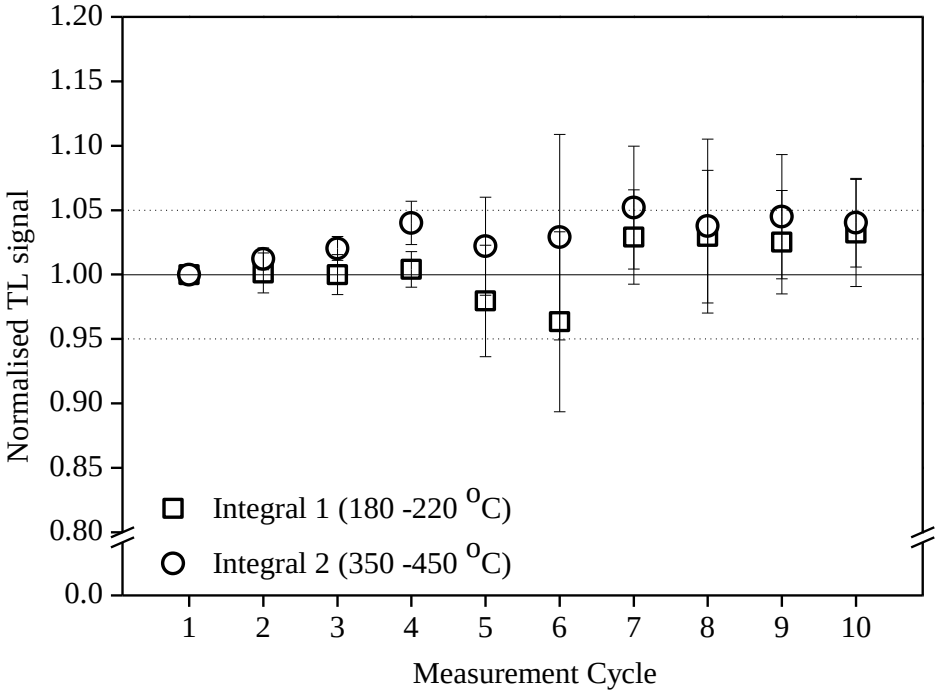

Fig. 10. Average (obtained on 12 aliquots) variation of integral TL output (180-220 ^{o}C – squares, respectively 350-450 ^{o}C- circles) of 0.5 P_2O_5 - 0.5 BaO glass freshly irradiated to a dose of 10 Gy upon re-using over a period of three months. All values have been normalized to the response obtained in the first measurement cycle. Dotted lines are meant as eye guides and represent 5% sensitivity variation. Error bars represent three times the standard error of the mean value.

In order to determine the thermal fading characteristics, twelve samples of 0.5 P_2O_5 - 0.5 BaO glass have been irradiated to a gamma dose of 10 Gy and were stored in dark conditions at room temperature for periods of time ranging from one day to four months. The 180-220 ^{o}C TL peak showed an average signal loss of 57 ± 2% over two days and a reduction up to 9 % ± 2% of the initial signal over the investigated time span. Thus, fading would hamper the use of this peak for dosimetric purposes.

For the high temperature peak, loss was observed for short time storage as well, but the signal reached a stable level at 75% of the instantaneous value (Fig. 11.). While it was found that low temperature peak is sensitive to light, there was no difference observed in the signal loss of the high temperature peak on exposure to light and in dark room conditions over a period of five days.

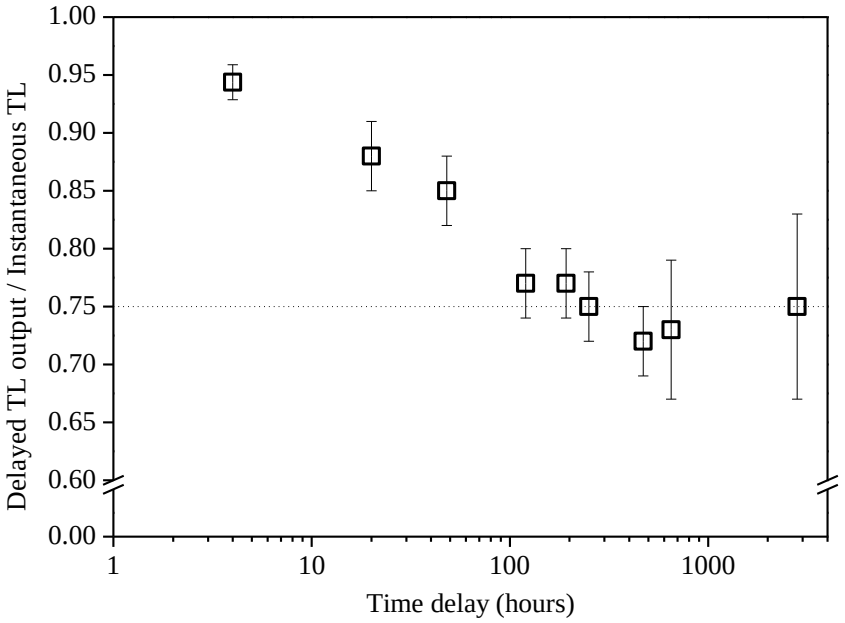

Fig. 11. Thermal fading characteristics of 0.5 P_2O_5 - 50 BaO glass. Data represents the average (12 samples) integral TL output (350-450 ^oC) as a function of storage time. Values are normalized to the luminescence signal measured immediately after irradiation. Error bars represent three times the standard error of the mean value.

For estimating the threshold dose and the minimum detectable dose the TL signal from a set of 10 not irradiated glass samples has been recorded.

The threshold dose was calculated by the expression

$$D_0=(B+2\sigma_B)\cdot$$

where F is the calibration factor expressed in Gy/TL, B is the mean TL signal obtained for the background and σ_B is the standard deviation of the background. For the high temperature peak (350-450 ^oC) a value of 0.2 Gy was obtained. The low limit of detection for this peak was estimated at 0.4 Gy at 95% confidence level according to equation (8) of Hirning et al. (1992) [38].

Optically stimulated luminescence signals were collected under continuous wave (CW) stimulation. Fig. 12. presents a comparison of the signal measured immediately after an irradiation with a dose of 10 Gy for the different glasses investigated. It can be seen that phosphate glass doped with BaO displays an intense fast decaying OSL signal, while Li glass modifier give rise to defects responsible only for modest optical luminescence signals. For 0.5 P_2O_5 -0.5 BaO a two exponential model fits acceptably well the OSL time decay data, the ratio of the corresponding cross sections involved being approximately 15 (value obtained on 12 aliquots).

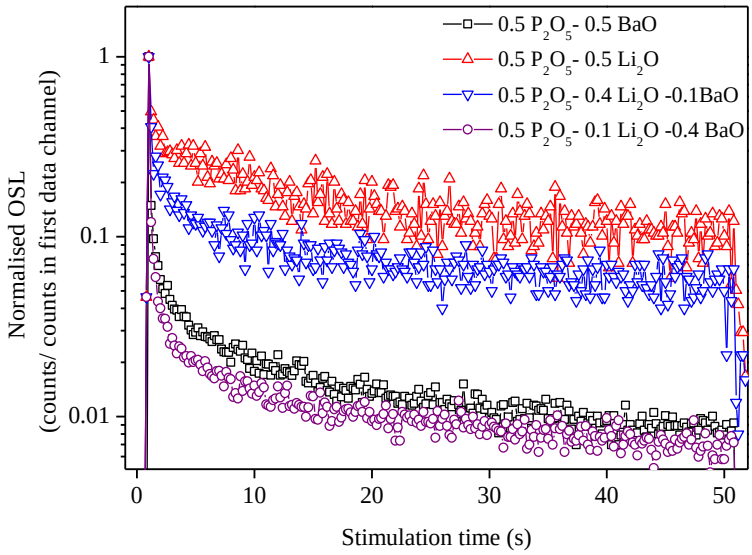

Fig. 12. Comparison of OSL decay curves of P_2O_5 glass systems doped with different concentrations of BaO and Li_2O. The signals have been registered immediately after 10 Gy of β irradiation. Each data point represents 0.3 seconds of stimulation; for the sake of visual comparison OSL signals of each analyzed sample have been normalized to the number of counts registered in first data channel.

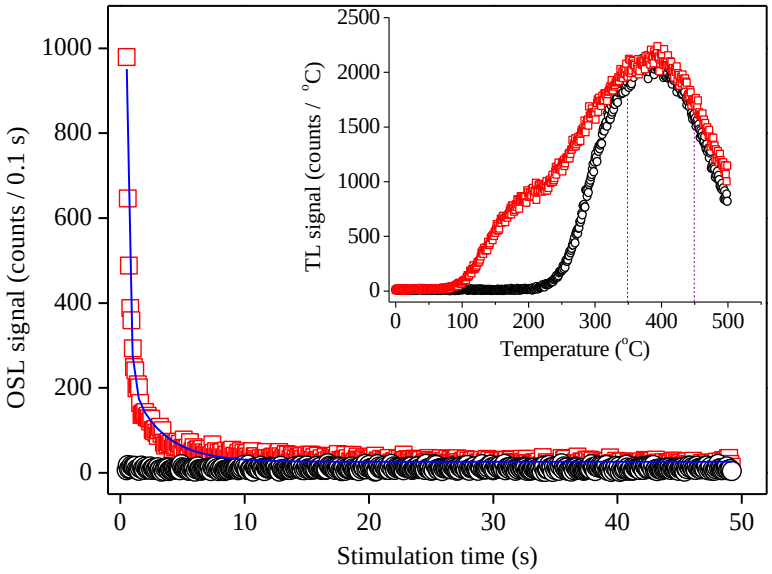

Fig. 13. Optically stimulated decay curve of 0.5 P_2O_5- 0.5 Ba O glass freshly irradiated (^{90}Sr-^{90} Y) to a dose of 10 Gy (squares). The fitted curve represents a double exponential decay ($I_{OSL} = a + I_1 \exp(-t \cdot \Phi \cdot \sigma_1) + I_2 \exp(-t \cdot \Phi \cdot \sigma_2)$). The OSL response of the same aliquot to the same dose recorded after a preheat of 10 s to 240 °C is represented as open cycles. The inset

presents the TL response of the same aliquot in the same measurement conditions (squares – instantaneous output; circles- glow curve recorded after a 10 s preheat @ 240 ^{o}C).

It was observed that OSL signals increase linearly with dose. However, a 100 hour delay between irradiation and measurement causes the signal to decrease to less than 50% the initial value (value obtained using 6 sub-samples), while a 10 second preheat at 240 ^{o}C, reduces the OSL signal to a negligible level. (Fig. 13.). Thus, it can be inferred that OSL signal in 0.5 P_2O_5 -0.5 BaO is correlated to the TL emission at about 200 ^{o}C.

CHAPTER 5

Vitreous glass system 0.5P2O5-xCdO-(0.5-x)Li2O

5.1. Sample preparation

$0.5P_2O_5$ x CdO (0.5-x)Li_2O glass system with $0 \leq x \leq 0.5$ mol%, was prepared by mixing $(NH_4)_2HPO_4$, $CdCO_3$ and Li_2CO_3 components of reagent grade purity. The samples were prepared by weighing suitable proportions of the components, powder mixing and mixture melting in sintered corundum crucibles at 1200^0 C for 1 h. The mixtures were put into the furnace directly at this temperature. The obtained glass-samples were quenched by pouring the molten glass on a stainless steel plate.

5.2. IR study of 0.5P2O5-xCdO-(0.5-x)Li2O glass system

Typical infrared spectra of studied the glasses are showed in Fig.14.

As seen from this figure, the frequencies of predominant absorptions are characterized by two broad peaks around 500 cm^{-1}, two weak peaks around 740 cm^{-1}, four peaks in the 900-1330 cm^{-1} region and a weak peak at 1641 cm^{-1}.

Because the majority of the bands are large and asymmetric, presenting also some shoulders, a deconvolution of the experimental spectra was made (Fig. 15.) using an ORIGIN 8.5 program with a Gaussian type function. This allowed us a better identification of all the bands and their assignments.

The band at about 470 cm^{-1} is assigned as the bending vibration of O–P–O units, $\delta(PO_2)$ modes of (PO_2^-)*n* chain groups, and the band at ~526 cm^{-1} is described as a fundamental frequency of (PO_4^{3-}) or as harmonics of P = O bending vibrations [21-23].

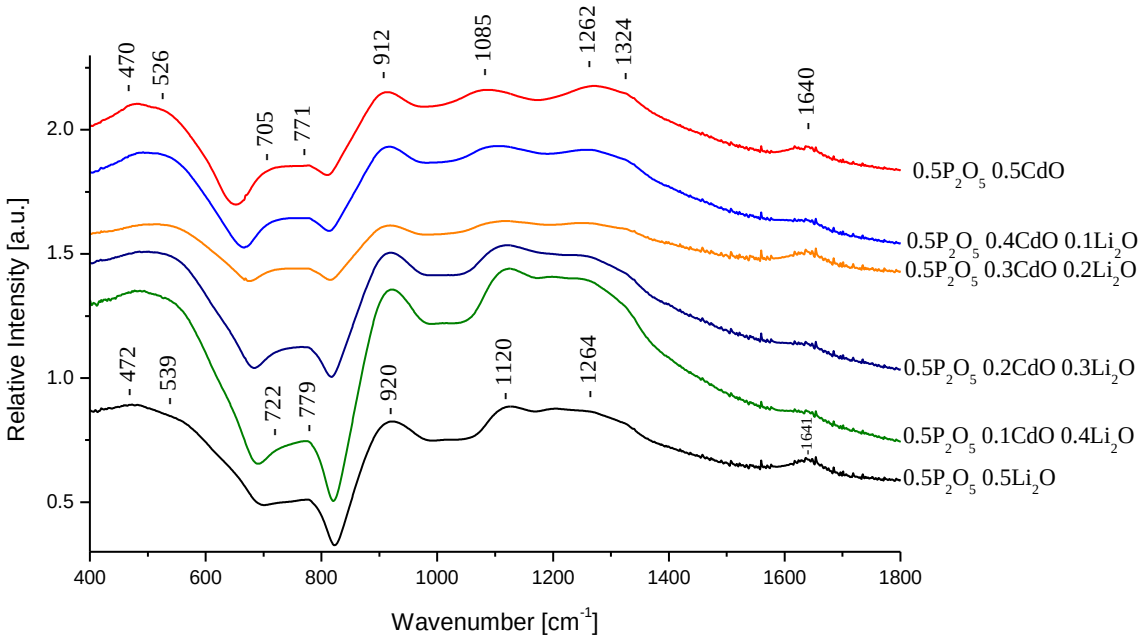

Fig.14. IR spectra of $0.5P_2O_5 \cdot xCdO\ (0.5\text{-}x)Li_2O$ glass system with $0 \leq x \leq 0.5$ mol%

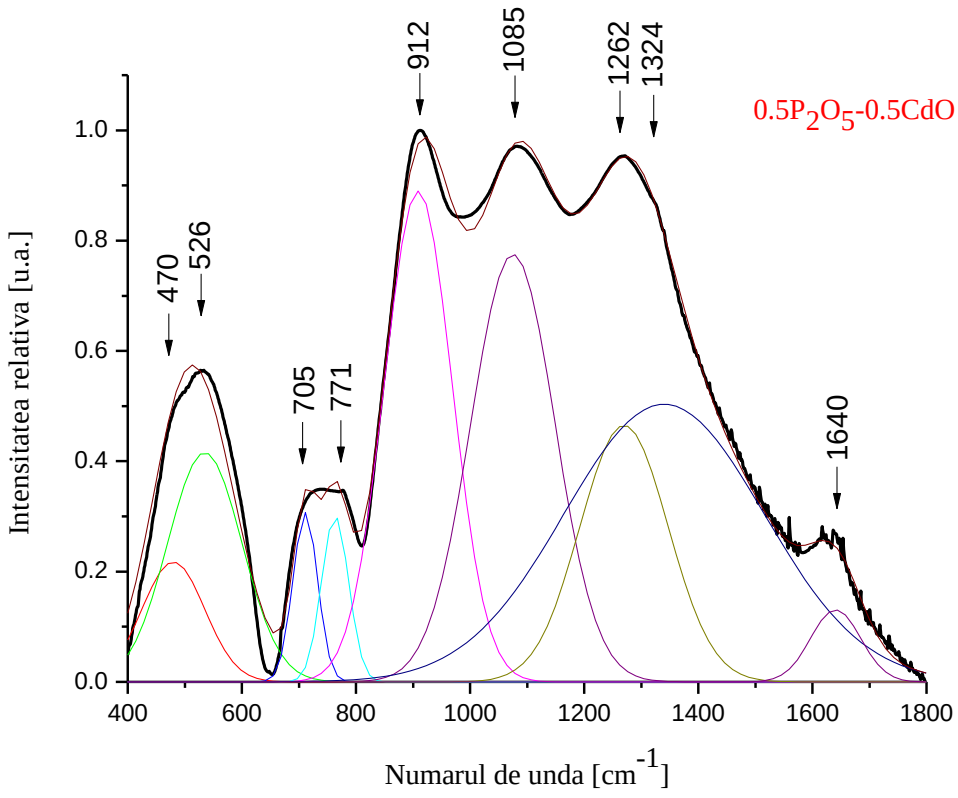

Fig.15. Deconvoluted IR spectra of $0.5P_2O_5 \cdot 0.5CdO$ glass using a Gaussian-type function

The band from 771 cm^{-1}, may be attributed to the symmetric stretching vibration of P–O–P rings [24]. The frequency of P–O–P bonds modifies with the increasing of Li_2O content due to its network modifier role and breakage of cyclic P–O–P bonds.

The absorption band at 912 cm^{-1} is attributed to asymmetric stretching vibration of P–O–P groups linked with linear metaphosphate chain [22, 23]. The band at ~1085 cm^{-1} is assigned to asymmetric stretching of PO_2^- group, $\upsilon_{as}(PO_2^-)$ modes [22, 23]. The considerable shift in the position of this band toward higher wavenumber, 1120 cm^{-1}, and the increase in its relative area (Fig. 16.) with increasing Li_2O content, may be considered as an indication for the formation of the terminal phosphate groups, PO_3^{2-}. The broad feature of the 1260 cm^{-1} band is attributed to the stretching of the doubly bonded oxygen vibration, υ_{as}(P = O) modes [24, 25].

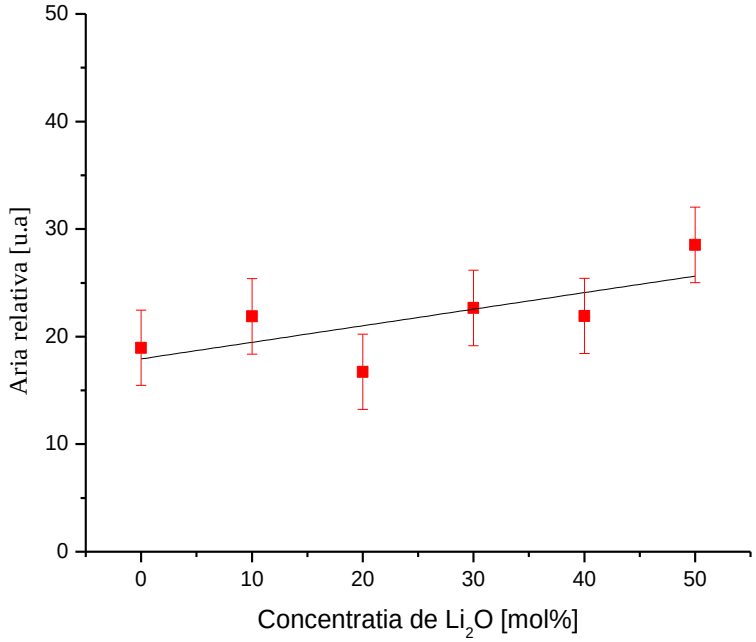

Fig. 16. The intensity of the band form 1085-1120cm^{-1} versus Li_2O mol% content. (The error bars are under 10% error limits)

The weak shoulder from 1324 cm^{-1} well evidenced at high CdO content may be due to a $P-O^-$ bond stretching vibrations combined with a lattice mode [25].

All spectra show a very weak band at 1640 cm^{-1} attributed to the bending vibrations of the free H_2O molecules [39].

5.3. Raman spectra of 0.5P2O5-xCdO-(0.5-x)Li2O system

Raman spectra of the investigated glasses (Fig. 17.) contain two significant adsorptions around ~700 cm^{-1} and ~1150 cm^{-1} [26,27]. The band from ~700 cm^{-1} corresponds to bridging stretching modes and that at ~1160 cm^{-1} is ascribed to the terminal P–O stretching vibrations. As in the case of IR spectra (Fig. 16.) the intensity of 700cm^{-1} band easily increases with Li_2O content. Beside these two intense bands in the Raman spectra of phosphate glasses, other supplementary bands under 600 cm^{-1} can be observed. These weak signals are due to the well-known boson peaks and to the complicated internal vibrations such as the skeletal deformation vibrations of phosphate chains and PO_3 deformation vibrations of pyrophosphate segments [28,29]. Thus the first band from ~340 cm^{-1} is attributed to skeletal deformation vibrations of phosphate chains and PO_3 deformation vibrations of pyrophosphate segments [29]. The second band at ~511 cm^{-1} corresponds to bending mode related to the cation motion and chain structure [30]. Other two weak bands appear at ~1012 cm^{-1} and ~1258 cm^{-1}, all the very high content of CdO. The band from ~1012 cm^{-1} is attributed to the symmetric stretching mode of O–P–O non-bridging oxygens, $(PO_2)_{sym}$, indicating the formation of Q^2 phosphate tetrahedra. The last band from ~1258 cm^{-1} is attributed to the symmetric stretch of P=O terminal oxygens, $(P=O)_{sym}$ [27,32].

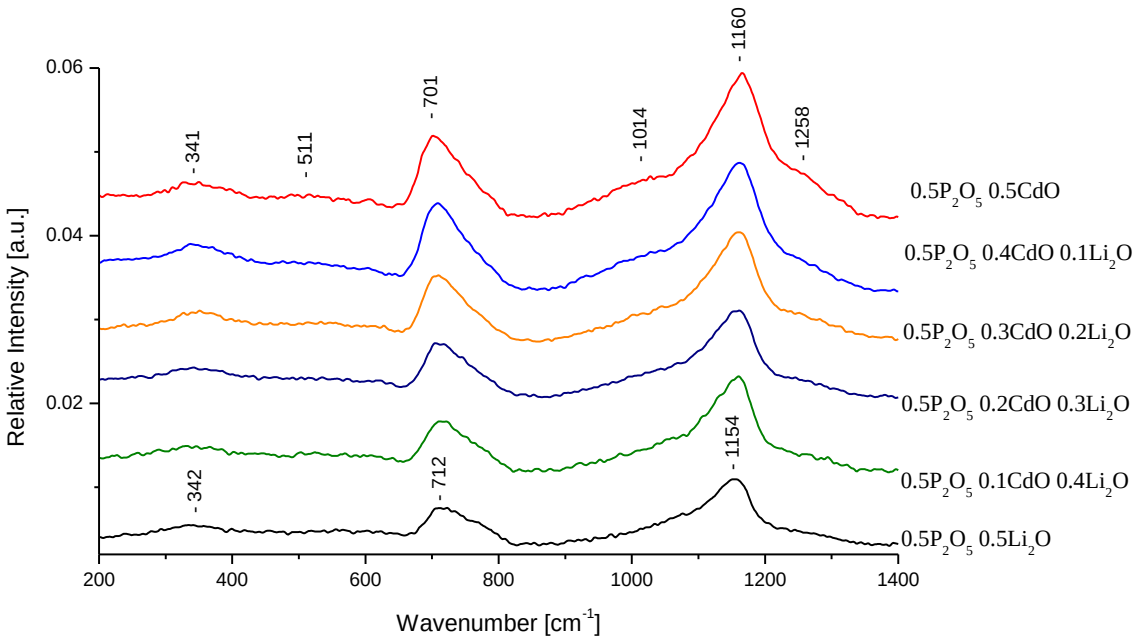

Fig.17. Raman spectra of $0.5P_2O_5$ xCdO $(0.5\text{-}x)Li_2O$ glass system with $0 \leq x \leq 0.5$ mol%

Weeks and Bray [40], observed that the band assigned to P=O terminal oxygens, centered at ~1390 cm^{-1}, shifts to ~1250 cm^{-1} with the increasing of the metal oxide from 20 to 50 mol% and became indistinguishable from the $(PO_2)_{asym}$ mode of a Q^2 tetrahedron. Its wavenumber is ascribed to an increase in average length of the P = O bond resulting from π-bond delocalization on the Q^3 tetrahedra [32].

In agreement with literature data [39-41], the IR and Raman spectra of Li_2O – P_2O_5, CdO – P_2O_5 and Li_2O – P_2O_5 – CdO glasses are dominated by the bands characteristic of different P – O type bonds.

The presence of Li^+ and Cd^{2+} cations in the phosphate network leads to shifting and intensity modification of some vibrational bands characteristic of some P–O groups. This is possible by the modification of covalency degree (and length) for P–O bonds and by favoring the appearance and disappearance of some phosphate structural groups [42].

5.4. ESR study of 0.5P2O5-xCdO-(0.5-x)Li2O glass system

The ESR spectra of typical gamma irradiated glass powder samples measured at room temperature are shown in Fig. 18. and are characterized by a doublet centered at g=2.023±0.002 ascribed to phosphorous oxygen hole center (POHC) [43].

The term POHC designates the defect responsible for a well-known ESR spectrum in irradiated phosphate glasses characterized by an approximately g tensor with g ~ 2.009 ± 0.002 and a small, nearly isotropic ^{31}P hyperfine interaction (~40 G) [44, 45]. The g value of the doublet is larger than that of the free spin, consistent with the nature of the hole center.

Weeks and Bray [40] demonstrated the existence of at least three ^{31}P hyperfine doublets of large splitting (70-140 G) in various phosphate glasses subjected to γ-radiation.

Crystalline phosphorus pentoxide P_2O_5 has a structure in which one of the oxygen ions is only bound to a phosphorus ion while the remaining three oxygen ions may either be bonded to another phosphorus ion as bridging oxygens (BO) or they can be at the end positions of the chain, as non-bridging oxygens (NBO).

In crystalline materials two types of oxygen vacancies can be formed, one type by the removal of an oxygen from the non-bridging site and one type by removal of an oxygen from the bridging site. These two types of oxygen vacancies might be expected to occur in P_2O_5 glass since, on average, the same number of BO and NBO per phosphorus ion are expected to be present in the glass as in the crystalline material. In order to clarify how the paramagnetic

centers responsible for the observed structures are generated by the damaging radiation, we have investigated the dependence of their intensity on the accumulated irradiation dose.

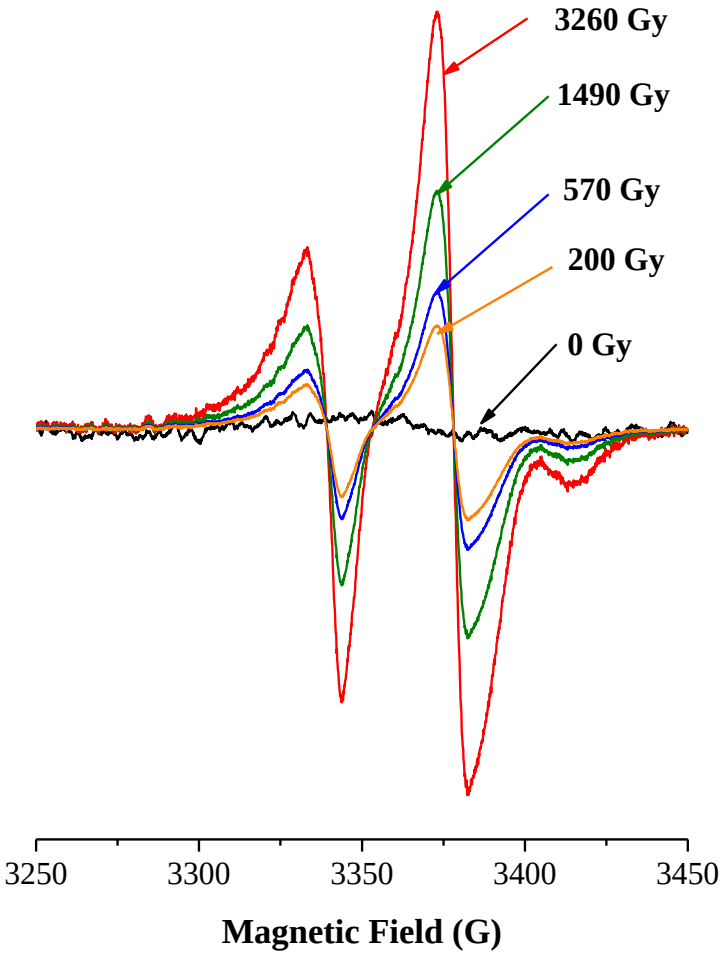

Fig. 18. ESR spectra of γ-irradiated $0.5P_2O_5$ - 0.2CdO – $0.3Li_2O$ sample at some absorbed doses

The signal intensity, or the integral of the EPR absorption spectrum, is proportional to the number of spins in the sample [46], and can therefore be used as estimation for the relative concentration of the paramagnetic species. The relative integral of the EPR absorption spectra intensities (proportionally with double integrate of EPR signal normalized on milligrams of sample) i.e. dose-response curves, was obtained by best least-squares fit to the parameters, given by the linear relationships: $I(D) = I_0 + I_1 D$ (Fig. 19.).The slope of this line is sufficiently high in order to these glass samples be elected as suitable for dosimetric purpose.

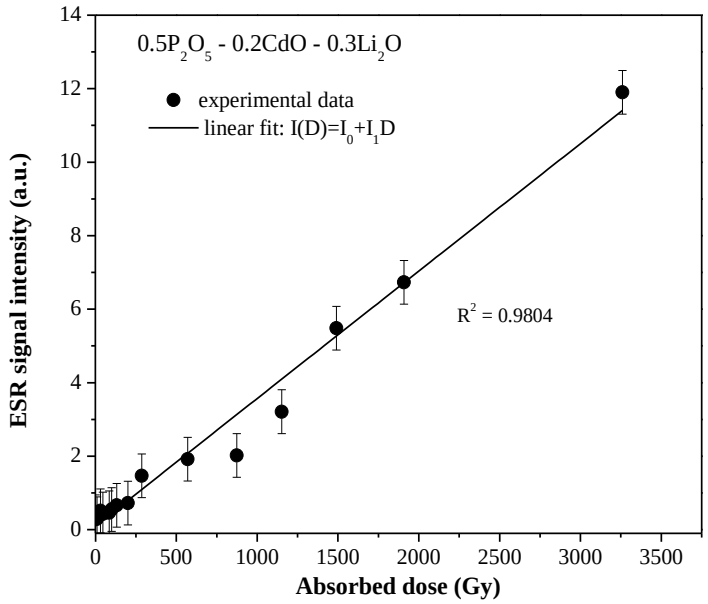

Fig. 19. Dose response relationship for $0.5P_2O_5$ - 0.2CdO – $0.3Li_2O$ glass as a function of the irradiated dose (errors bars are provided with 6% error limits)

CHAPTER 6

Vitreous glass system 0.5P2O5-xBaO-(0.5-x)K2O

6.1. Sample preparation

The starting materials for obtain $0.5P_2O_5$-xBaO-(0.5-x)K_2O glass system with $0 \leq x \leq$ 50 mol% were $(NH_4)_2HPO_4$, $BaCO_3$ and K_2CO_3 of reagent grade purity. The samples were prepared by weighing suitable proportions of the components, powder mixing and mixture melting in sintered corundum crucibles at 1200 °C for one hour. The mixture was put into the furnace directly at this temperature. The obtained glass-samples were quenched by pouring the molten glass on a stainless steel plate.

6.2. IR spectra of $0.5P_2O_5$-xBaO-(0.5-x)K_2O system

Typical infrared spectra of studied glasses are shown in Fig.20. As seen from this figure, the frequencies of predominant absorption peaks are characterized by two broad peaks near 500 cm^{-1}, two weak peak around 740 cm^{-1}, five peaks in the 890-1410 cm^{-1} region and a weak peak around 1625 cm^{-1}.

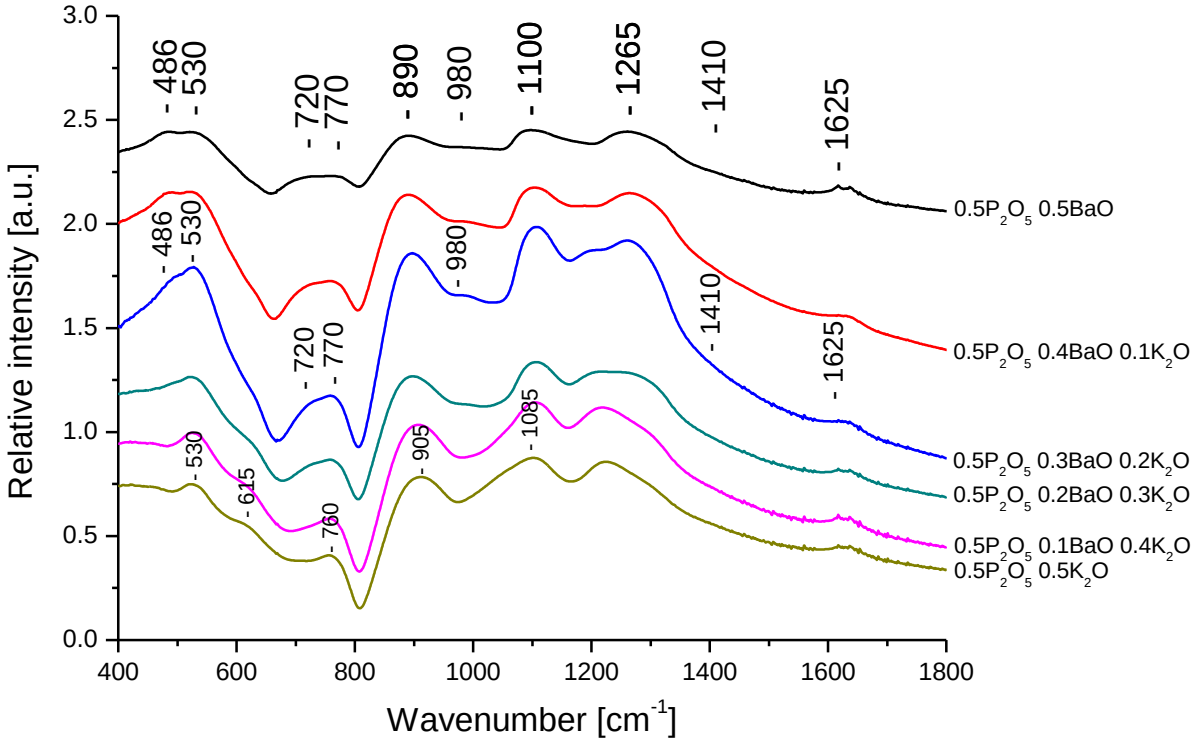

Fig. 20. IR spectra of $0.5P_2O_5$-xBaO-(0.5-x)K_2O glass system with $0 \leq x \leq 0.5$ mol%

Because the majority of the bands are large and asymmetric, presenting also some shoulders, a deconvolution of the experimental spectra was made (Fig. 21., Fig. 22.) using an ORIGIN 8.5 program with a Gaussian type function. This allowed us a better identification of all the bands and their assignments.

The band at about 486 cm^{-1} is assigned as the bending vibration of O–P–O units, $\delta(PO_2)$ modes of $(PO_2^-)n$ chain groups and he decreases in intensity and disappears with increasing concentration of K_2O.. The band at ~530 cm^{-1} is described as a fundamental frequency of (PO_4^{3-}) or as harmonics of P = O bending vibrations [21–23].

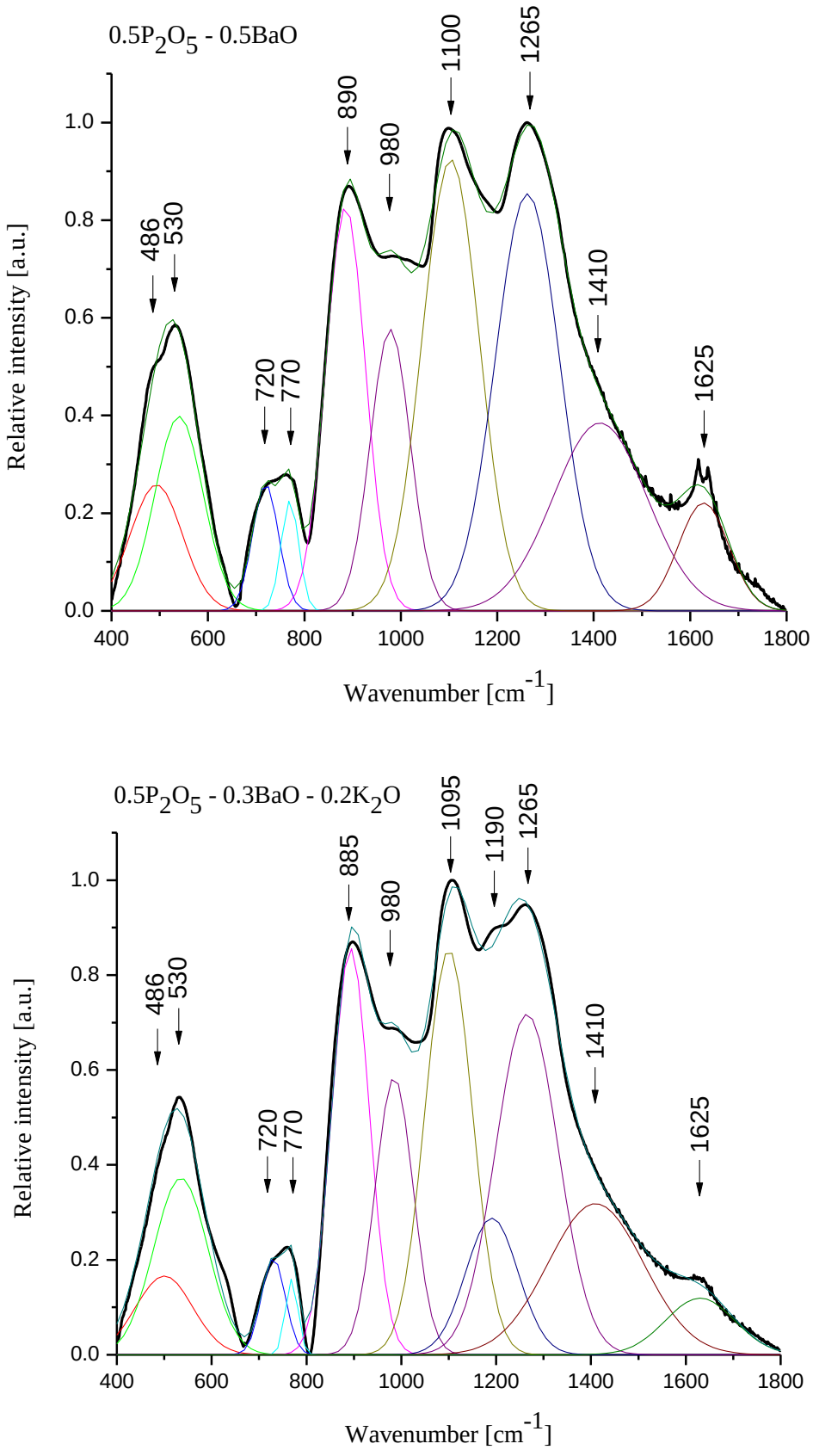

Fig. 21. Deconvoluted IR spectra of $0.5P_2O_5$-xBaO-(0.5-x)K_2O glass system using a Gaussian-type function for x=0.5% mol şi x=0.3% mol

Increasing concentration of K_2O the band from about 720 cm^{-1} assigned to symmetric stretching vibrations in P-O-P groups disappears, appearing a new band at 615 cm^{-1} due to stretching vibrations of different harmonics of the bonds O=P-O [24]. The band from 770 cm^{-1}, may be attributed to the symmetric stretching vibration of P–O–P rings [24]. The frequency of P–O–P bonds modifies with the increasing of K_2O content due to its network modifier role and breakage of cyclic P–O–P bonds.

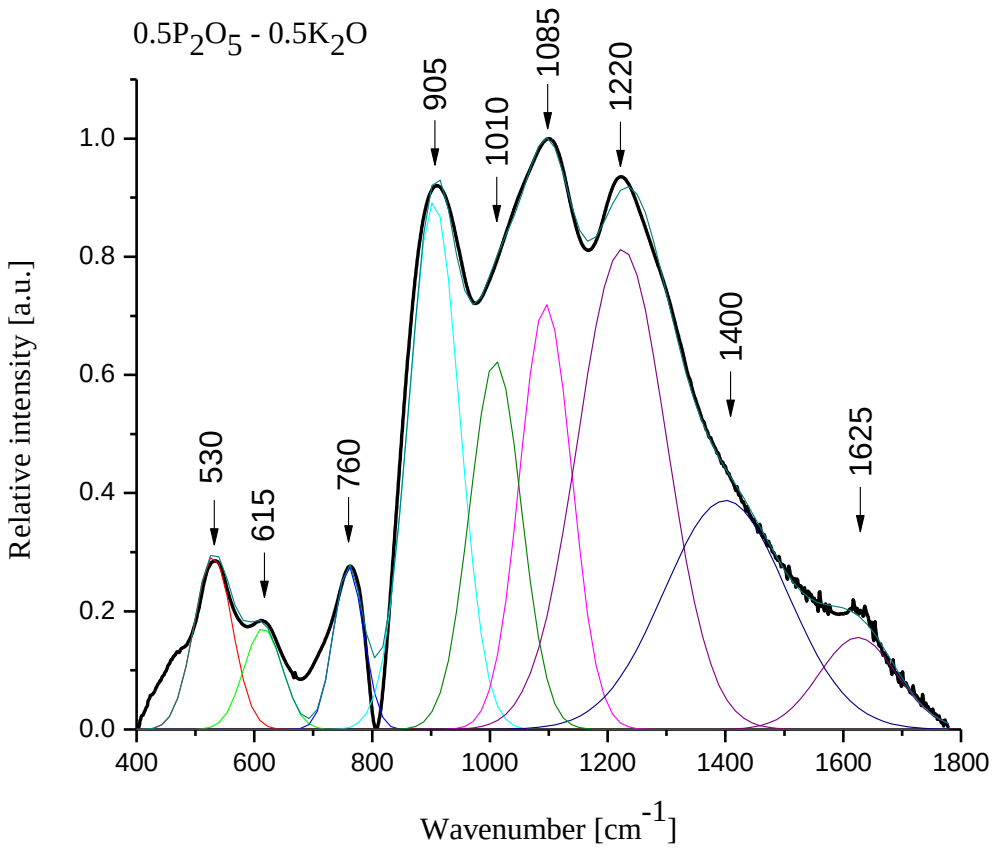

Fig. 22. Deconvoluted IR spectra of $0.5P_2O_5$-$0.5K_2O$ glass using a Gaussian-type function

The absorption band at 890 cm^{-1} is attributed to asymmetric stretching vibration of P–O–P groups linked with linear metaphosphate chain [22, 23]. The band from 980 cm^{-1} can be assigned to asymmetric stretching vibration of PO_4^{3-} structural group [22].

The band at ~1100 cm^{-1} is assigned to asymmetric stretching of PO_2^- group, $\upsilon_{as}(PO_2^-)$ modes [22,23]. The considerable shift in the position of this band toward higher wavenumber, (from 1085 cm^{-1} to 1100 cm^{-1}) and the increase in its relative area (Fig. 23.) with increasing

BaO content, may be considered as an indication for the formation of the terminal phosphate groups, PO_3^{2-}.

We observe a new band at 1190 cm^{-1} attributed to asymmetric stretching vibrations of PO_2^-groups in the spectrum of $0.5P_2O_5$-0.3BaO-$0.2K_2O$ glass.

The broad feature of the 1265 cm^{-1} band is attributed to the stretching of the doubly bonded oxygen vibration, υ_{as}(P = O) modes [24, 25]. The weak shoulder from 1410 cm^{-1} can be assigned to asymmetric stretching vibration of double bonded P=O [25, 32].

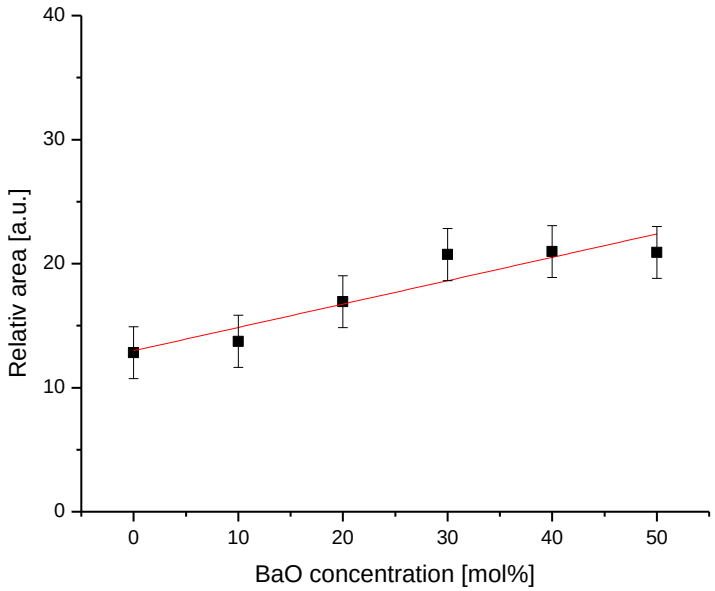

Fig. 23. The intensity of the band form 1085-1100cm^{-1} versus Li_2O mol% content. (The error bars are under 10% error limits)

All spectra show a very weak band at 1625 cm^{-1} attributed to the bending vibrations of the free H_2O molecules [39].

6.3. Raman spectra of $0.5P_2O_5$-xBaO-(0.5-x)K_2O system

Raman spectra of the investigated glasses (Fig. 24.) contain two significant adsorptions around ~700 cm^{-1} and ~1150 cm^{-1} [26,27]. Beside these two intense bands in the Raman spectra of phosphate glasses, other supplementary bands under 600 cm^{-1} can be observed. These weak signals are due to the well-known boson peaks and to the complicated

internal vibrations such as the skeletal deformation vibrations of phosphate chains and PO_3 deformation vibrations of pyrophosphate segments [28,29].

For a better identification of all the bands and their assignments a deconvolution of the experimental spectra was made using an ORIGIN 8.5 program with a Gaussian type function.

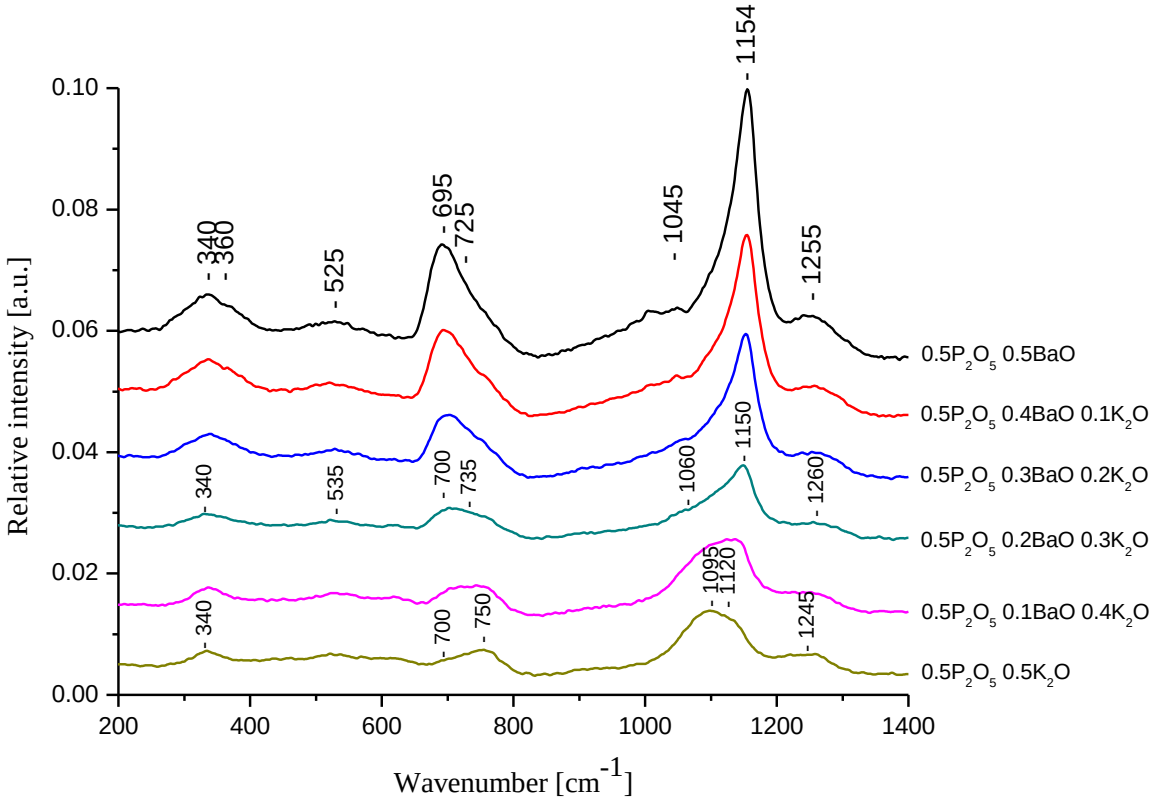

Fig. 24. Raman spectra of $0.5P_2O_5$-xBaO-(0.5-x)K_2O glass system

The first band from ~340 cm^{-1} is attributed to skeletal deformation vibrations of phosphate chains and PO_3 deformation vibrations of pyrophosphate segments [29]. In the case of $0.5P_2O_5$-0.5BaO glass appears a weak band at 360 cm^{-1} assigned to deformation vibrations of phosphate polyhedral (PO_4). The band at ~525 cm^{-1} corresponds to bending mode related to the cation motion and chain structure [30].

The band from ~695 cm^{-1} corresponds to the symmetric stretching mode of P-O-P bridging oxygens. The band from 725 cm^{-1} attributed to the symmetric stretching mode of O-P-O linkages shifts to 750 cm^{-1} with the increasing of K_2O content. At ~1045 cm^{-1} we have a band ascribed to the terminal P–O stretching vibrations.

Other two weak bands appear at ~1154cm^{-1} and ~1255 cm^{-1}, all the very high content of BaO. The band from ~1154 cm^{-1} is attributed to the symmetric stretching mode of O–P–O non-bridging oxygens, $(PO_2)_{sym}$, indicating the formation of Q^2 phosphate tetrahedra.

We observe a new band at 1095 cm^{-1} attributed to symmetric stretching vibrations of PO_3^{2-}groups in the spectrum of $0.5P_2O_5$-$0.5K_2O$ glass.

The last band from ~1258 cm^{-1} is attributed to the symmetric stretch of P=O terminal oxygens, $(P=O)_{sym}$ [27,32].

Weeks and Bray [40], observed that the band assigned to P=O terminal oxygens, centered at ~1390 cm^{-1}, shifts to ~1250 cm^{-1} with the increasing of the metal oxide from 20 to 50 mol% and became indistinguishable from the $(PO_2)_{asym}$ mode of a Q^2 tetrahedron. Its wavenumber is ascribed to an increase in average length of the P = O bond resulting from π-bond delocalization on the Q^3 tetrahedra [32].

The presence of Ba^+ and K^{2+} cations in the phosphate network leads to shifting and intensity modification of some vibrational bands characteristic of some P–O groups. This is possible by the modification of covalency degree (and length) for P–O bonds and by favoring the appearance and disappearance of some phosphate structural groups.

6.4. Thermoluminescence study of $0.5P_2O_5$-xBaO-(0.5-x)K_2O glass system

Thermoluminescence emissions have been registered under a controlled heating rate of 5 ^oC/s immediately after 25 Gy of β irradiation.

Simple phosphate glasses exhibited no TL signals. Thus, it can be inferred that the observed TL peaks correspond to different defects generated by the modifier ions (Ba^+, respectively K^{2+}) inserted into the glass network.

At least two peaks can be easily observed in the case of $0.5P_2O_5$ -0.5BaO (Fig. 25.) freshly irradiated glass, one centered on 200 ^oC and a higher temperature peak at about 400 ^oC, while in the case of 0.5 P_2O_5 - 0.5 K_2O (Fig. 26) the TL peak is centered at about 280 ^oC.

In the case of $0.5P_2O_5$ - x BaO - (0.5-x) K_2O glass systems with $10 \leq x \leq 40$ mol% TL emissions are consisting of the above-mentioned peaks overlapping.

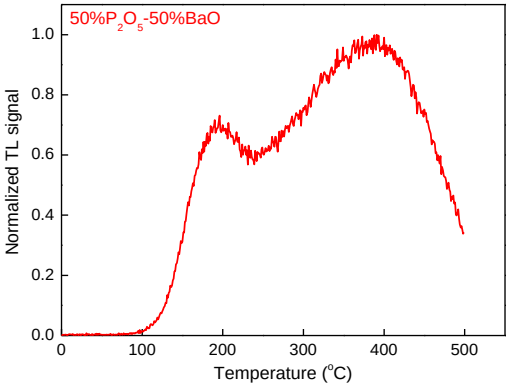

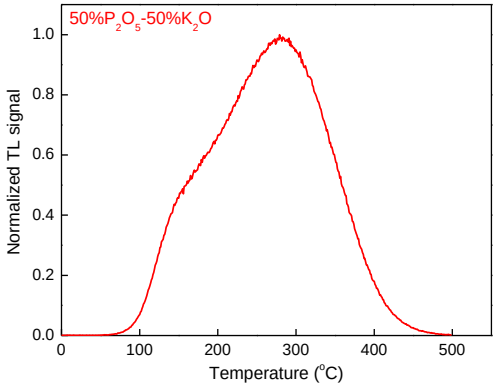

Fig. 25. TL glow curves of 0.5 P_2O_5 - 50 BaO

Fig. 26. TL glow curves of $0.5P_2O_5$-$0.5K_2O$

The dose response of TL signals for 0.5 P_2O_5 - 0.5 K_2O glass is presented in Fig. 27. All measurements have been performed on a single aliquot for each glass specimen, as it was observed that the process of recording the TL signal (ramp heating to 500 ^oC) reduces all signals to a negligible level (3% of the response recorded after an irradiation of 10Gy).

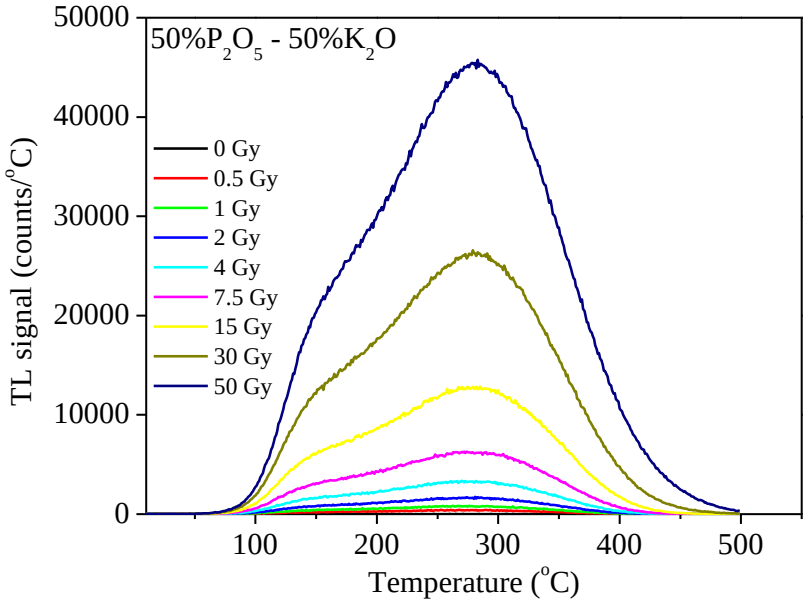

Fig. 27. TL glow curves of 0.5 P_2O_5 – 0.5 K_2O glass freshly irradiated (^{90}Sr- ^{90}Y) to doses ranging from 0 to 50 Gy

A very good linear dependence ($R^2 > 0.99$) of the integral TL signal with dose can be observed for dosimetric peak of $0.5P_2O_5$ - $0.5K_2O$ up to at least 50Gy (Fig. 28.).

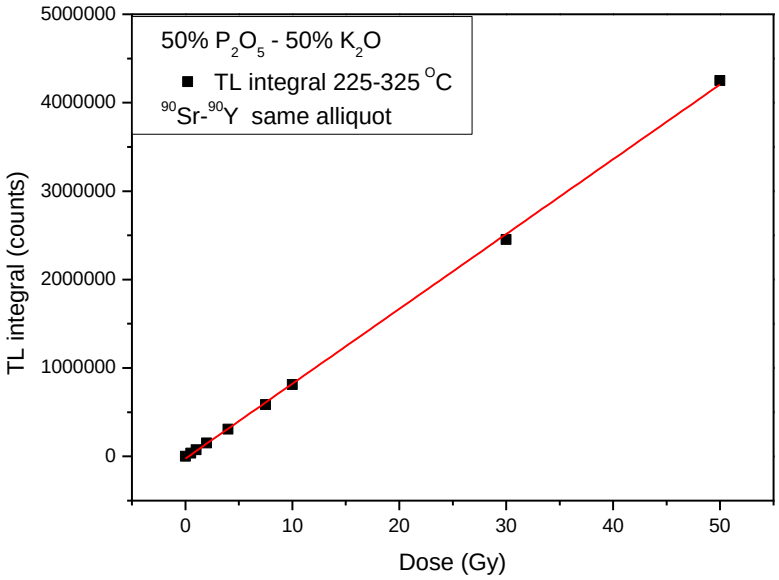

Fig. 28. Integral TL response (225 -325 ^{o}C) as function of given dose.

Reproducibility tests have been carried on one aliquot, this aliquot being repeatedly irradiated and heated to 500 ^{o}C. The average behavior of one aliquot over 10 measurement cycles is presented in Fig. 29.. None of the investigated aliquots showed a specific sensitization or desensitization trend.

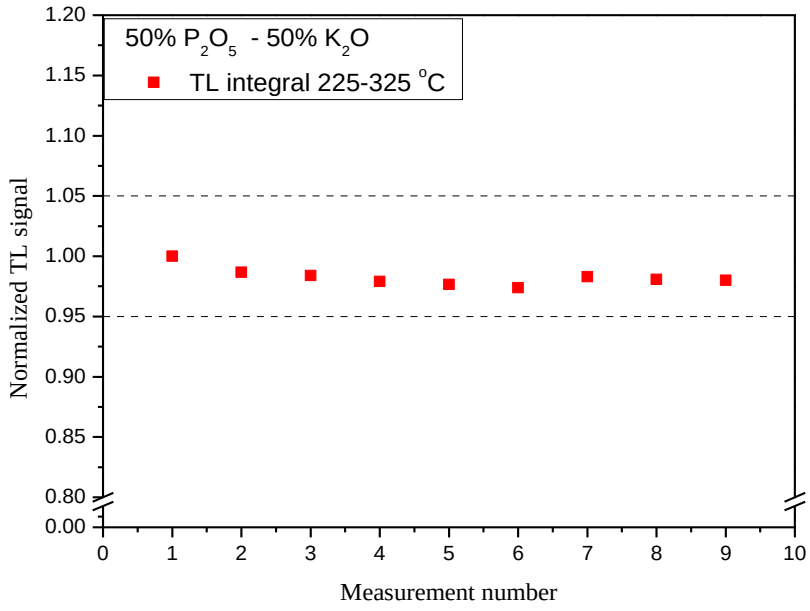

Fig. 29. Variation of integral TL output (2250-325 ^{o}C) of 0.5 P_2O_5 - 0.5 K_2O glass freshly irradiated to a dose of 10 Gy.

SELECTED CONCLUSIONS

In Chapter 4 has been studied the effect of incorporating modifier BaO and Li_2O oxides in phosphate glass matrices on thermoluminescence and optically stimulated luminescence properties of these materials. It was concluded that the presence of both Ba^{+2} and Li^{+1} ions leads to the generation of thermoluminescence and optically stimulated luminescence signals upon irradiation.

The TL emission at 400 ^oC of P_2O_5 - BaO, however, was found to display encouraging dosimetric properties in the high dose range, well above the saturation limit of traditional materials: good linearity up to at least 100 Gy (R^2>0.99), acceptable batch homogeneity (<10% standard deviation) and reproducibility (<5% deviation for 10 measurement cycles performed over the course of several months). Although the signal was found to be affected by fading, on long term it was found that it reached a stable level.

The characteristic bands from IR and Raman spectra of the investigated glasses were assigned to the stretching and bending vibrations of the P-O-P and O-P-O groups, respectively, in the Q^n formalism.

In Chapter 5 was presented an IR, Raman and ESR study of the P_2O_5-CdO-Li_2O glass system. IR and Raman spectra allowed us to identify the structural units from the studied phosphate glasses. The presence of network modifier Li^+ and Cd^{2+} cations manifest by shifting and the intensity modifications of some characteristic phosphate bands changing the covalency degree (and length) of P–O bands and favoring the appearance and disappearance of some structural groups.

The linear relationship between absorbed dose and ESR signal intensity in the range of 100Gy to 2.5kGy suggests the possibility of used this glass system for dose measurements.

Chapter 6 present IR, Raman study and thermoluminescence properties of $0.5P_2O_5$-xBaO-(0.5-x) K_2O glass system, where $0 \leq x \leq 0.5$ mol%. The characteristic bands from IR and Raman spectra are dominated by vibrational bands specific phosphate groups. For a better identification of all the bands and their assignments was made a deconvolution of the experimental spectra using an ORIGIN 8.5 program with a Gaussian type function.

The good linearity up to at least 50 Gy (R^2>0.99) obtained from thermoluminescence measurements suggests the possibility of using this glass system for medical dosimetry.

SELECTED REFERENCES

[1.] I. Ardelean, Introducere în studiul materialelor oxidice cu structură vitroasă, Cluj-Napoca, (2002).

[2.] P. Baltă, Tehnologia sticlei, Ed. Didactică şi Pedagogică, Bucureşti, (1984).

[3.] A. E. R. Westman, Moderns Aspects of the Vitreous State, Butterworths, London, (1960).

[4.] I. Cădariu, Chimia fizică, Ed. Tehnică, Bucureşti, vol. 1, (1967).

[5.] H. Rawson, Inorganic Glass-Forming System, Academic Press, London, (1967).

[6.] J. F. Ducel, J. J. Videau, K. J. Suh, J. Senegas, J. Alloys Comp. 188 157 (1992); Phys. Chem. Glasses 35, 10 (1994).

[7.] E. Kordes, Z. Anorg. Allgem. Chem. 241, 1 (1939).

[8.] R. K. Brow, J. Non-Cryst. Solids, 263&264, 1(2000).

[9.] F. Liebau, in: M. O'Keefe, A. Novrotsky (Eds.), Structure and Bonding in Crystals II. Academic Press, New York, 197 (1981).

[10.] J. R. Van Wazer, Phosphorus and its Compounds, vol. 1, Interscience, New York (1958).

[11.] Spectroscopic methods in mineralogy / EMU Notes Mineral., 6/ Budapest : Eötvös Univ. Press (2004).

[12.] T. Iliescu, S. Cântă Pânzaru, D. Maniu, R. Grecu, S. Aştilean, Aplicații ale spectroscopiei vibraționale, Casa Cărții de Știință, Cluj- Napoca, (2002).

[13.] I. Ardelean, R. Ciceo-Lucăcel, Fizica şi tehnologia materialelor oxidice. Lucrări practice. Ed. Univ. „Babeş-Bolyai" Cluj-Napoca, (2000).

[14.] A. Efimov, J. Non-Cryst. Solids 253, 95 (1999).

[15.] I. Ardelean, C. Andronache, C. Câmpean, P. Păşcuță, Mod. Phys. Lett. B 45, 1811 (2004).

[16.] P. Y. Shih, J. Ding, S. Lee, Mat. Chem. Phys. 80, 391 (2003).

[17.] C. Furetta, P.S. Weng, Operational Thermoluminescence Dosimetry, World Scientific Publishing (1998).

[18.] B.M. Yavorsky, A.A. Pinsky, Fundamentals of Physics, vol.2 cap 79.2. Mir Publishers Moscow (1975).

[19.] M. Oncescu, I. Panaitescu, Dozimetria şi ecranarea radiațiilor Röentgen şi Gamma, Editura Academiei Române (1992).

[20.] **C. Ivascu**, A. Timar Gabor, O. Cozar, L. Daraban, I. Ardelean, J. Molec. Struct., 993, 249 (2011).

[21.] J. Ahmed, M. Lewis, J. Olsen, J.C. Knowles, Biomaterials, 25, 491(2004).

[22.] H. Doweidar, Y.M. Moustafa, K. El-Egili, I.Abbas, Vibr.Spectrosc., 37, 91(2005).

[23.] P. Bergo, S.T. Reis, W.M. Pontuschka, J.M. Prison, C.C. Motta, J.Non-Cryst.Solids, 336, 159(2004).

[24.] M. Scagliotti, M. Villa, G. Chiodelli, J.Non-Cryst.Solids, 93, 350(1987).

[25.] D.A. Magdas, O. Cozar, I. Ardelean, L. David, J.Opt.Adv.Mater., 9(3), 730(2007).

[26.] P.Y. Shih, J.Y. Ding, S.Y. Lee, Mater.Chem.Phys., 80, 391(2003).

[27.] I. Ardelean, D. Rusu, C. Andronache, V. Ciobotă, Mater. Leters, 61, 3301(2007).

[28.] M.E. Lines, A.E. Miller, K. Nassau, K.B. Lyous, J.Non-Cryst.Solids, 89, 163(1987).

[29.] J. Koo, B. Bac, H. Na, J.Non-Cryst. Solids, 212, 173(1997).

[30.] A.M. Milankovic, A. Gajovic, A. Santic, D.E. Day, J. Non-Cryst. Solids, 289, 204 (2001).

[31.] **C. Ivascu**, L. Daraban, O. Cozar and I. Ardelean, 30th European Congress on Molecular Spectroscopy, Firenze, Italy, 28 aug. – 3 sep. 2010

[32.] J.J. Hudgens, R.K. Brow, D.R. Tallant, S.W. Martin, J. Non-Cryst. Solids, 223, 21(1998).

[33.] Timar-Gabor, **C. Ivascu**, S. Vasiliniuc, L. Daraban, I. Ardelean, C. Cosma, O. Cozar, App. Rad. and Isotopes, 69, 780 (2011).

[34.] **C. Ivascu**, L. Dărăban, A. Timar Gabor, N. Vedeanu, O. Cozar, 4th Conference on Advanced Spectroscopies on Biomedical and Nanostructured Systems, Cluj-Napoca, Romania, 4 – 7 sep. 2011

[35.] C. Furetta, M. Prokic, R Salamon,V. Procik, G. Kitis, Nuclear Instruments in Physics Research A, 456, 411(2001).

[36.] R. Chen, IRPA Regional Congress on Radiation Protection in Central Europe, 20-01, 1(2001).

[37.] C. Furetta, P.S. Weng, World Scientific Publishing, ISBN: 981-02-3468-6, 252(1998).

[38.] C.R. Hirning,. Health Physics, 62, 223(1992.)

[39.] A.N. Regos, R.C. Lucacel, I. Ardelean, J. Mater Sci. 46 (2011) 7313.

[40.] R.A. Weeks, P.J. Bray, J. Chem Phys. 48 (1968) 5

[41.] N. Kerkouri, M. Haddad, M. Et-tabirou, A. Chahine, L. Laânab, Physica B 406 (2011) 3142.

[42.] **C. Ivascu**, G. Damian, L. Daraban, I. Ardelean, O. Cozar, 31th European Congress on Molecular Spectroscopy, Cluj – Napoca, Romania, 26 – 31 aug. 2012

[43.] **C. Ivascu**, I.B. Cozar, L. Daraban, G. Damian, J. Non-Cryst. Solids, 359, 60 (2013)

[44.] Z.M. Da Costa, W.M. Pontuschka, J.M. Giehl, C.R. Da Costa ,J. Non-Cryst. Solids 352 (2006) 3663.

[45.] V. Simon, I. Ardelean, O. Cozar, S. Simon, J. Mat. Sci. Letters 15 (1996) 784.

[46.] G. Damian, Talanta 60 (2003) 923.